

Direct torque control of 4 phase 8/6 switched reluctance motor drive for constant torque load

Srinivas Pratapgiri* , Prasad Polaki Venkata Narsimha

Department of Electrical Engg., University College of Engineering, Osmania University, Hyderabad 515005, India

(Received January 13 2011, Accepted January 11 2012)

Abstract. The Switched Reluctance Motor (SRM) Drives have attracted the attention of many researchers in the recent past because of advantages like simple mechanical structure, adaptability to harsh environments like coal mining etc. But it has one main disadvantage of high torque ripple due to its double saliency structure. The Direct Torque Control (DTC) technique can minimize the torque ripple by regulating torque within specified hysteresis band. This paper presents the Direct Torque Control of 4 phase 8/6 Switched Reluctance Motor fed through an asymmetrical converter. A four phase asymmetrical converter has total 81 Space voltage vectors. So like the conventional DTC applied to ac motor, 8 Space voltage vectors are sufficient to apply DTC technique to SRM. The Direct Torque Control of SRM is simulated in MATLAB/ SIMULINK for constant torque load. The performance of the drive mainly in terms of torque ripple is analyzed with new set of space vectors.

Keywords: direct torque control, switched reluctance motor, torque ripple

1 Introduction

Switched Reluctance Motor (SRM) has salient poles on both stator and rotor with concentrated winding on the stator and no winding on the rotor. As rotor does not have any winding, it can withstand high temperatures and can rotate at very high speeds. The SRM achieves high torque levels at low peak currents by using small air gaps. The SRM drives are inherently adjustable speed drives. SRM has attracted many researchers in the recent years because of the simple construction and low manufacturing cost. Because of the availability of low cost power electronic switches and fast computing motor specific controllers like Digital signal processors, the conventional variable AC/DC machines are now replaced by SRMs in applications like coal mining, electric vehicles, compressors, electric traction, washing machines etc. The main drawback of the motor is that it has highly non-linear torque-position characteristics and a torque ripple is high, which causes noise and vibrations^[10].

Different techniques have been proposed in the past to minimize torque ripple. The most popular electronic method is based on the optimization of control principles, which include the supply voltage, turn-on and turn-off angles of the converter and current levels. But this method has the disadvantage that it leads to reduction in the overall torque^[5]. Venkatesha et al. in [9] proposed the torque ripple minimization by suitably profiling the phase currents. But the method is quite involved and the computation time required is high. The Neuro-Fuzzy control technique proposed by Henriques et al. in [4] adds a compensating signal to the PI controller. But the stability of this method depends on the selection of suitable value of the stopping time. Torque ripple minimization of 8/6 SRM using fuzzy logic controller for constant dwell angles has been analyzed in [12].

Zhen et al. in [15] has reduced the ripples in torque by employing a torque controller and fuzzy logic controller. Torque controller is used for limiting the phase current and fuzzy logic controller for adjusting the

* Corresponding author. Tel.: +91-040-2709 8628. E-mail address: srinivasp.eedou@gmail.com.

turn-on and turn-off angles. But this method is limited to low speed region. DTC proposed in [8] uses the concept of short flux pattern. But it has the disadvantage of requirement of new winding topology, which is expensive and also inconvenient. In [1, 2] a novel DTC technique is applied to 3-phase 6/4 SRM in which the difference between conventional DTC applied to ac machines and the new DTC proposed to SRM has been elaborately discussed. DTC of 3 phase SRM has been also presented in [3, 11] along with simulation results. The low speed and high speed operation of 6/4 SRM drive is observed in [7] using DTC method. DTC of 4 phase 8/6 SR motor is analyzed only in [6, 14].

This paper presents DTC based 4 phase 8/6 SRM by selecting a suitable set of 8 Space voltage vectors. The DTC of SRM drive is simulated for constant torque load to observe the steady state and transient performance of the drive. It is observed that the torque is maintained within the set hysteresis band. This paper with new set of space vectors shows a significant improvement in the torque performance of DTC based SRM compared to the DTC scheme shown in [3]. There is a considerable reduction in the torque ripple in the present study.

The paper is organized as follows. Section 2 describes the mathematical equations of SRM and principle of DTC. The block diagram of the DTC based SRM is explained in Section 3. Simulation and analysis of results are presented in Section 4. Conclusions are presented in Section 5.

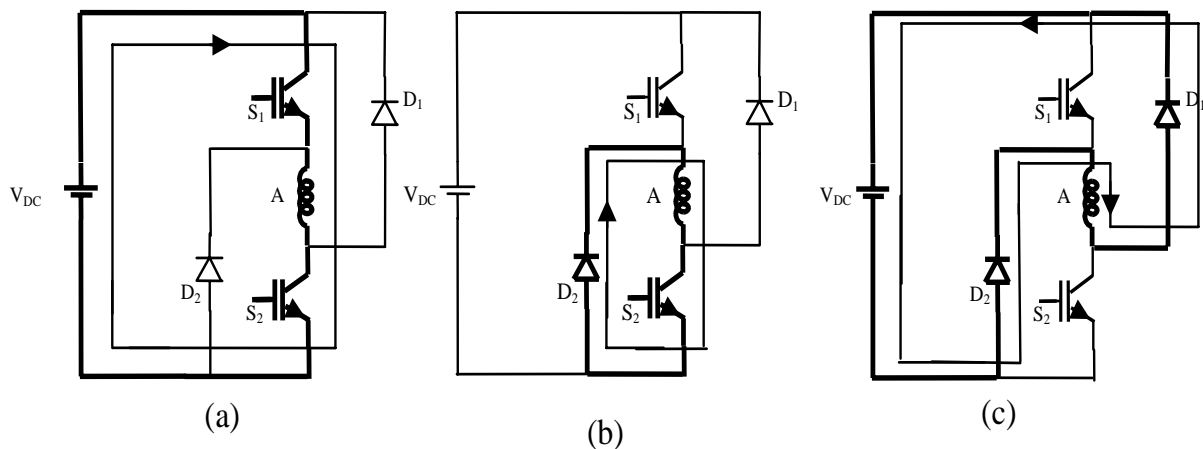


Fig. 1. SRM phase voltage states

2 Direct torque controller

The mathematical equations of DTC [2] as applied to SRM are discussed as below. The motor torque output can be found using the electromagnetic equation

$$v = Ri + \frac{d\psi(\theta, i)}{dt}, \quad (1)$$

where $\psi(\theta, i)$ is the nonlinear function of phase flux linkage as a function of rotor position θ and current i . Expanding the above equation, results in Eq. (2)

$$v = Ri + \frac{\partial\psi(\theta, i)}{\partial i} \frac{di}{dt} + \frac{\partial\psi(\theta, i)}{\partial\theta} \frac{d\theta}{dt}. \quad (2)$$

Thus the equation for the power flow can be written as

$$vi = Ri^2 + i \frac{\partial\psi(\theta, i)}{\partial i} \frac{di}{dt} + i \frac{\partial\psi(\theta, i)}{\partial\theta} \frac{d\theta}{dt}. \quad (3)$$

Now the effective power flow P_{eff} from the electric source can be defined as

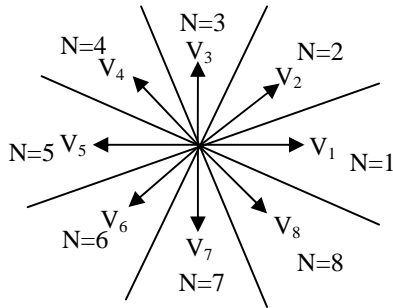


Fig. 2. Definition of SRM motor voltage vectors for DTC

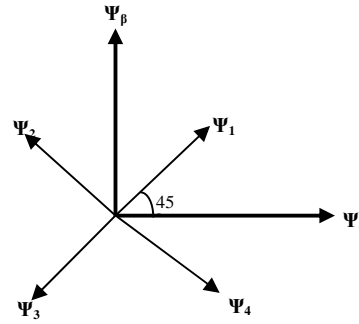


Fig. 3. Definition of - axis for motor voltage

$$P_{\text{eff}} = ei,$$

where $e = (v - Ri)$.

Thus in a differential time dt , the differential electrical energy dW_e transferred from the source is given by

$$dW_e = eiddt. \tag{4}$$

To find an expression for the motor torque production, the energy equation is written as

$$dW_e = dW_m + dW_f, \tag{5}$$

where dW_m and dW_f are the differential mechanical energy and field energy respectively. The field energy can be separated into its constituent components as shown in Eq. (6)

$$dW_f = \frac{\partial W_f}{\partial i} di|_{\theta=\text{const}} + \frac{\partial W_f}{\partial \theta} d\theta|_{i=\text{const}}. \tag{6}$$

From the consideration of the stored field energy it can be shown that^[13]:

$$dW_e = i \frac{\partial \psi(\theta, i)}{\partial i} di|_{\theta=\text{const}} + i \frac{\partial \psi(\theta, i)}{\partial \theta} d\theta|_{i=\text{const}}, \tag{7}$$

$$dW_f|_{\theta=\text{const}} = i \frac{\partial \psi(\theta, i)}{\partial i} di|_{\theta=\text{const}}. \tag{8}$$

By substitution of Eq. (6) into Eq. (7) it can be found that

$$dW_m = i \frac{\partial \psi(\theta, i)}{\partial \theta} d\theta - \frac{\partial W_f}{\partial \theta} d\theta. \tag{9}$$

The instantaneous torque is defined by

$$T = \frac{dW_m}{d\theta}. \tag{10}$$

Thus by substituting Eq. (10) into Eq. (9) the expression for the instantaneous torque production of an SR motor phase can be written as

$$T = i \frac{\partial \psi(\theta, i)}{\partial \theta} - \frac{\partial W_f}{\partial \theta}. \tag{11}$$

This is a rarely used variant of conventional torque equation. Due to saturation in the SR motor, the influence of the second term in Eq. (11) is negligible. Therefore, by using this approximation, the following equation for torque production may be derived as

$$T \approx i \frac{\partial \psi(\theta, i)}{\partial \theta}. \tag{12}$$

In SRM, unipolar drives are normally used and thus the current in a motor phase is always positive. Hence, from Eq. (12) the sign of the torque is directly related to the sign of $\frac{\partial \psi}{\partial \theta}$. In other words to produce a positive torque, the stator flux amplitude must increase relative to the rotor position, whereas to produce a negative torque the change in stator flux should decrease with respect to the rotor movement. A positive value of $\frac{\partial \psi}{\partial \theta}$ may be defined as “flux acceleration”, whereas a negative value of $\frac{\partial \psi}{\partial \theta}$ may be defined as “flux deceleration”[2]. Hence, a new SR motor control technique^[2] is defined as follows:

- (i) The stator flux linkage vector of the motor is kept at constant amplitude.
- (ii) Torque is controlled by accelerating or decelerating the stator flux vector.

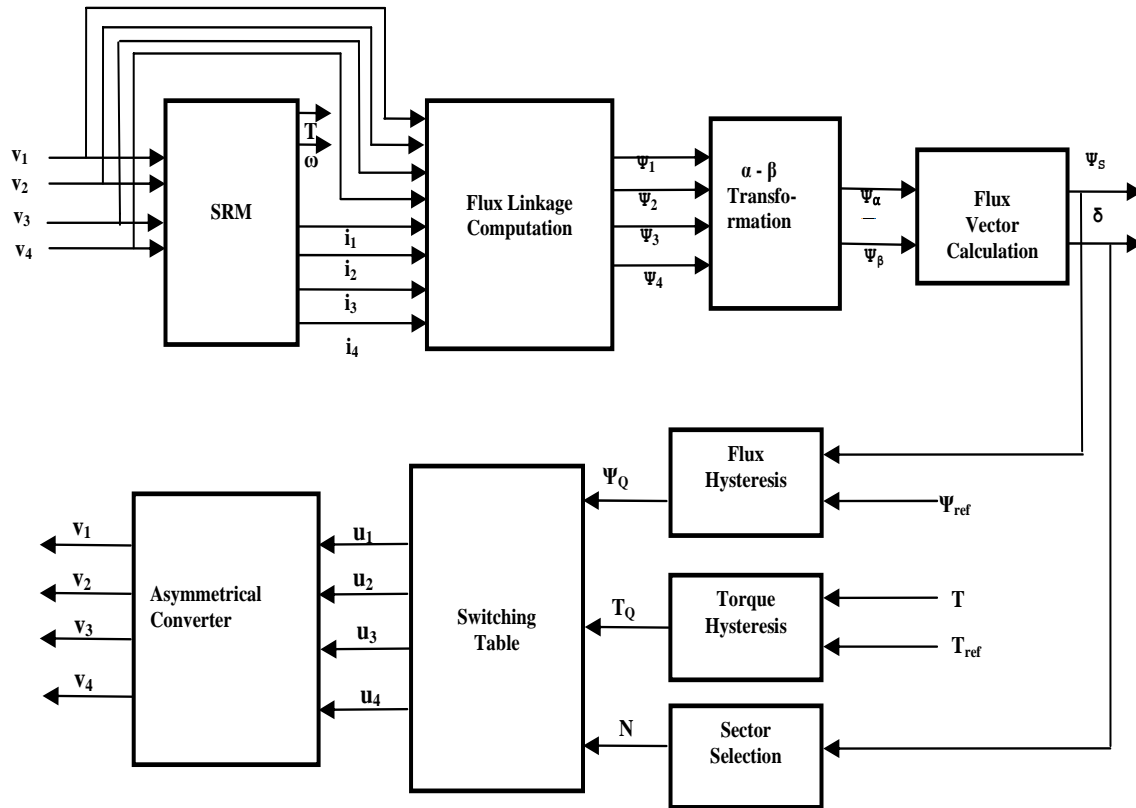


Fig. 4. Block diagram of DTC based SRM drive

The objective of control technique (i) is achieved similarly to the conventional DTC applied to ac machines by selecting an appropriate Space voltage vector. As in conventional ac machine DTC, the stator flux variation will have the same directional variation as the voltage vector and a change in amplitude that is proportional to the magnitude of the voltage and the time interval of application. The objective (ii) is also achieved similarly to the conventional ac motor DTC because the torque is increased or decreased by acceleration or deceleration of the stator flux vector relative to the rotor movement^[2].

Table 1. Switching Table of space voltage vectors

N		1	2	3	4	5	6	7	8
$\psi_Q = 1$	TQ = 1	V2	V3	V4	V5	V6	V7	V8	V1
	TQ = 0	V7	V8	V1	V2	V3	V4	V5	V6
$\psi_Q = 0$	TQ = 1	V3	V4	V5	V6	V7	V8	V1	V2
	TQ = 0	V6	V7	V8	V1	V2	V3	V4	V5

Asymmetrical converter is popularly used for the SRM drives. Due to its structure, asymmetrical converters have more switching states than the conventional converters. As can be seen in Fig. 1, each motor phase can have three possible voltage states for a unidirectional current. Fig. 1 (a) shows that when both devices in converter are turned 'On'. In this case positive voltage is applied to the motor phase. The voltage state for a given phase is defined as 1. When current is flowing and one device is turned 'Off', a zero voltage loop occurs and the state is defined as 0. This is shown in Fig. 1 (b). Fig. 1 (c) shows that when both devices are turned 'Off', the current freewheels through the diodes. In this case negative voltage is experienced by the motor phase and the state is defined as -1. The 4 phase asymmetrical converter can have a total of 81 possible Space voltage vectors. However in order to apply DTC to SRM, eight equal amplitude voltage vectors that are separated by $\pi/4$ radians are sufficient. The space voltage vector states are shown in Fig. 2. These voltage state vectors are defined to lie in the center of eight zones $N = 1, 2, \dots, 8$, where each zone has a width of $\pi/4$ radians.

One of the eight possible states is chosen at any one time in order to keep the stator flux linkage and the motor torque within hysteresis bands. As in the conventional DTC scheme, if the stator flux linkage lies in the k th zone, the magnitude of the flux can be increased by using the switching vectors V_{k+1} and V_{k-1} and can be decreased by using the vectors V_{k+2} and V_{k-2} . Hence, whenever the stator flux linkage reaches its upper limit in the hysteresis band, it is reduced by applying voltage vectors which are directed toward the center of the flux vector space and vice-versa. As detailed previously, the torque is controlled by an acceleration or deceleration of the stator flux relative to the rotor movement. Hence, if an increase in torque is required, voltage vectors that advance the stator flux linkage in the direction of rotation are selected. This corresponds to selection of vectors V_{k+1} and V_{k+2} for a stator flux linkage in the k th zone. If a decrease in torque is required, voltage vectors are applied which decelerate the stator flux linkage vector. This corresponds to the vectors V_{k-1} and V_{k-2} in the k th zone. Hence a switching table for controlling the stator flux linkage and motor torque can be defined as shown in Tab. 1, where $\Psi_Q = 1$ & $\Psi_Q = 0$ indicate increase and decrease in the flux-linkages respectively and $T_Q = 1$ & $T_Q = 0$ indicate increase and decrease in torque respectively.

In order to resolve the individual phase flux vectors into a single stator flux linkage vector, the flux vectors for the four phase SRM are transformed onto a stationary orthogonal two axis reference frame [6] as shown in Fig. 3.

$$\begin{aligned}\psi_\alpha &= \psi_1 \cos 45^\circ - \psi_2 \cos 45^\circ - \psi_3 \cos 45^\circ + \psi_4 \cos 45^\circ, \\ \psi_\beta &= \psi_1 \sin 45^\circ + \psi_2 \sin 45^\circ - \psi_3 \sin 45^\circ - \psi_4 \sin 45^\circ, \\ \psi_s &= \sqrt{(\psi_\alpha^2 + \psi_\beta^2)}, \quad \delta = \arctan \left[\frac{\psi_\beta}{\psi_\alpha} \right].\end{aligned}\quad (13)$$

where Ψ_s is the flux vector, δ is the angle of the flux vector and $\Psi_1, \Psi_2, \Psi_3, \Psi_4$ are the flux-linkages of the four phases.

Specifications of SRM:

Aligned Inductance	110 mH
Unaligned Inductance	10 mH
Stator Resistance	0.3
Inertia	0.0082 Kg.m ²
Friction	0.001 N.m.s
Maximum Current	30 A
Voltage	120 V
Maximum Flux-linkage	0.3 V.s

3 Block diagram of DTC

Fig. 4 shows the block diagram of the proposed DTC based 4 phase 8/6 SRM drive. The flux in each phase is calculated by flux linkage computation block. The output of the flux linkage computation block is

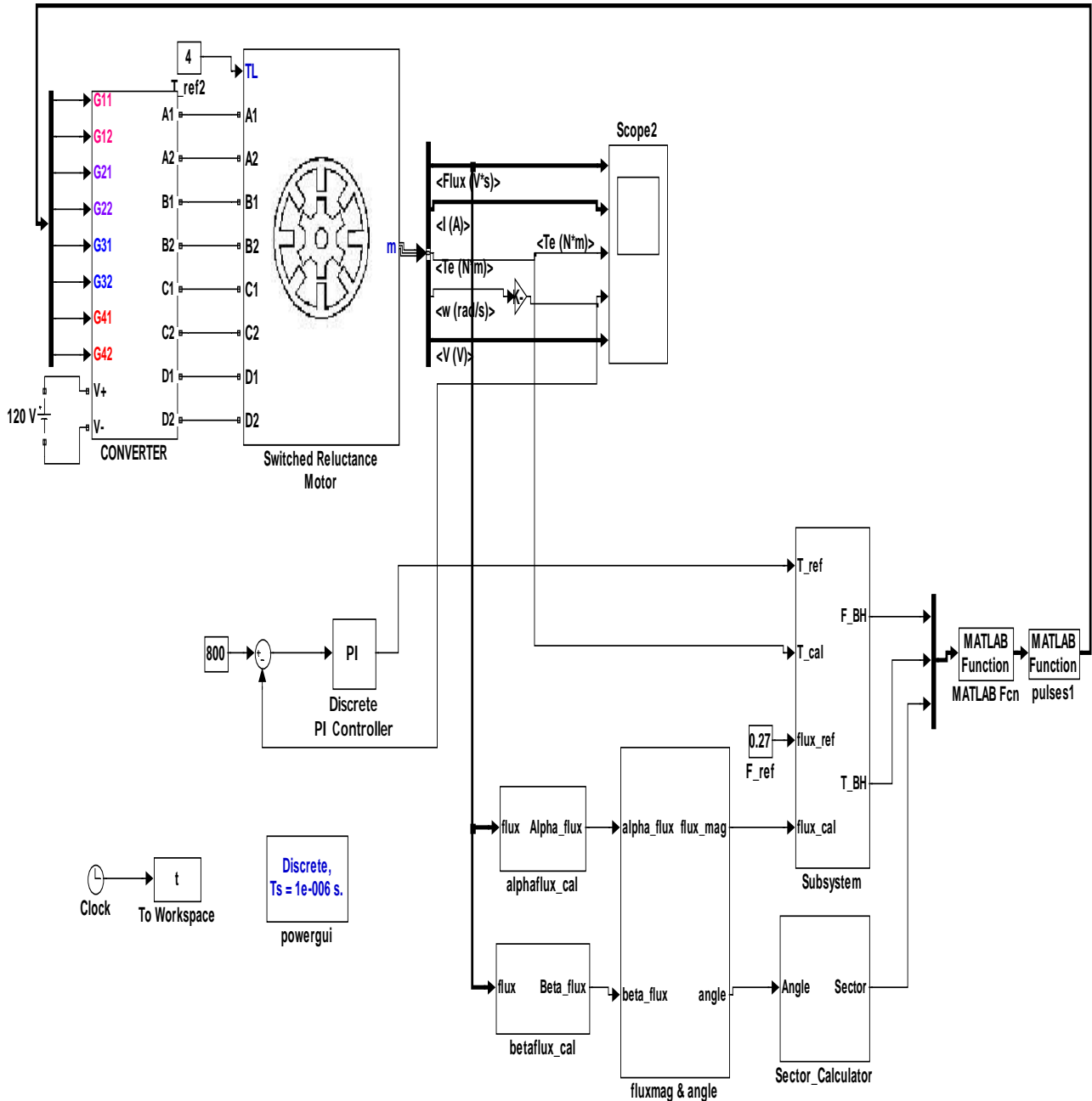


Fig. 5. Simulation model of 4 phase 8/6 SRM with DTC

given to the $\alpha - \beta$ block where the flux in 4 phases are converted into 2 phases. The magnitude Ψ_s and angle δ of the flux vector are calculated by flux vector calculation block. The flux vector magnitude Ψ_s and the motor torque T calculated from the motor are then fed into flux and torque hysteresis blocks, together with the reference values of flux and torque. The hysteresis blocks outputs the flux and torque increase or decrease command Ψ_Q and T_Q depending on the current flux and torque magnitudes relative to the hysteresis bands. The switching table and asymmetrical converter apply the suitable voltage vectors to the SRM windings.

4 Simulation and results

The DTC of 4 phase 8/6 SRM is modeled and simulated in MATLAB /SIMULINK. Fig. 5 shows the simulation model of 8/6 SRM with direct torque controller. The model consists of 4 phase 8/6 SRM, asym-

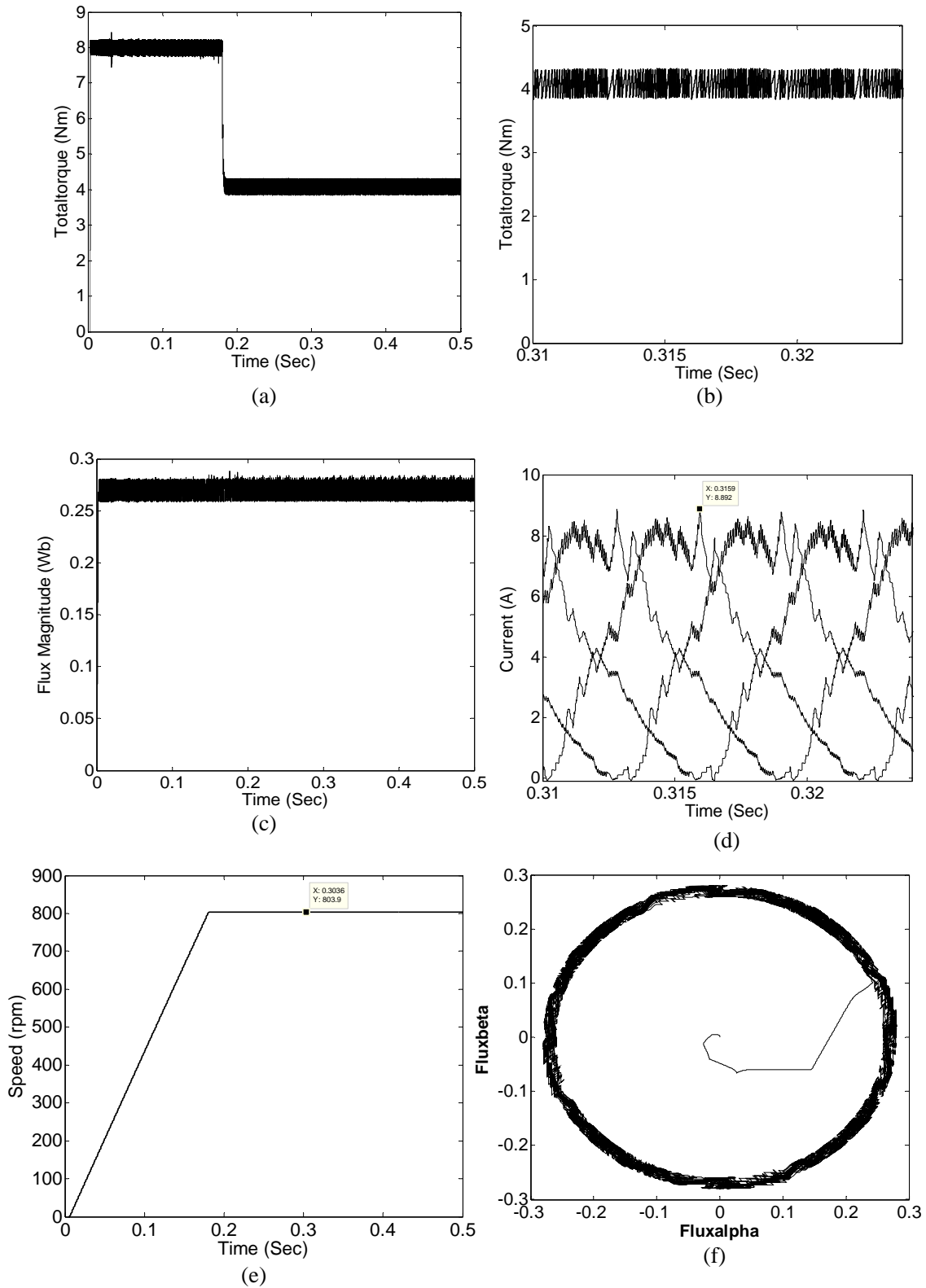


Fig. 6. Simulation waveforms DTC based SRM (a) Total torque (b) Total torque in steady state (c) Flux magnitude (d) Phase currents (e) Speed (f) Flux vector trajectory

metrical converter, DTC controller and PI Controller. In this simulation test, the motor reference flux is taken as 0.27 Wb and a load torque is taken as 4 Nm. The hysteresis bands were defined to be 0.02 Wb and 0.4 Nm for the flux linkage and torque respectively. The DTC scheme is simulated by selecting the following set of 8 Space voltage vectors.

$$\begin{aligned} V_1 &= (-1010), & V_2 &= (-1 - 111), & V_3 &= (0 - 101), & V_4 &= (1 - 1 - 11), \\ V_5 &= (10 - 10), & V_6 &= (11 - 1 - 1), & V_7 &= (010 - 1), & V_8 &= (-111 - 1). \end{aligned}$$

The performance of the DTC based SRM drive is analyzed for a constant load torque of 4 Nm at a reference speed of 800 rpm. Actual speed is compared with the reference speed and error is given to a PI controller. The output of PI controller is the reference torque. The maximum value of PI controller output is 8 Nm whenever the speed is less than the reference speed. When the speed reaches the reference value the PI controller output is equal to the load torque. Fig. 6 (a) shows the total torque response over the entire simulation time. During acceleration period the torque is maintained at 8 Nm by following a hysteresis band of 0.41 Nm till the steady state is reached. When the steady state is reached the torque developed by the motor is maintained at the load torque by following a hysteresis band of 0.41 Nm. Thus the torque ripple is minimized in the steady state and during acceleration period. The calculated torque ripple is 10%. Fig. 6 (b) shows the total torque response in steady state. Fig. 6 (c) shows the magnitude of the flux vector. The total flux is maintained at 0.27 Wb by following a set hysteresis band of 0.02 Wb. The current waveforms of all the four phases in the steady state are shown in Fig. 6 (d). The maximum current and average current of each phase are 8.9 A and 4.13 A respectively. Fig. 6 (e) shows speed response. The steady state speed is maintained constant at 803 rpm. Fig. 6 (f) shows the trajectory of the flux vector.

5 Conclusions

In this paper the control of 4 phase 8/6 SRM is analyzed with Direct Torque Control technique. The torque is controlled directly through the control of magnitude of the flux linkage and the change in speed of the stator flux vector. The performance of direct torque controlled SRM drive is analyzed by selecting a suitable set of 8 Space voltage vectors for constant load torque. It is observed that torque is maintained within set hysteresis band of 10% of rated torque during acceleration and in the steady state. The torque ripple is 10% in the steady state. A further study can be made on the reduction of phase current variations by maintaining the torque and flux within their respective bands.

References

- [1] A. Cheok, P. Hoon. A new torque control method for switched reluctance motor drives. **in:** *26th Annual conference of the IEEE Industrial Electronics Society, IECON 2000*, 2000, 387–392.
- [2] A. Cheok, Y. Fukuda. A new torque and flux control method for switched reluctance motor drives. *IEEE Transactions on Power Electronics*, 2002, **17**(4): 543–557.
- [3] H. Guo. Considerations of direct torque control for switched reluctance motors. **in:** *Proceedings of the 2006 IEEE International Symposium on Industrial Electronics, ISIE*, 2006, 2321–2325.
- [4] L. Henriques, L. Rolim, et al. Torque ripple minimization of switched reluctance drive using a neuro-fuzzy compensation. *IEEE Transactions on Magnetics*, 2000, **36**(5): 3592–3594.
- [5] I. Husain. Minimization of torque ripple in srm drives. *IEEE Transactions on Industrial Electronics*, 2002, **49**(1): 28–39.
- [6] B. Jeong, K. Lee, et al. Direct torque control for the 4-phase switched reluctance motor drives. **in:** *Proceedings of the 2005 IEEE International Conference on Electrical Machines and Systems, ICEMS 2005*, 2005, 524–528.
- [7] R. Jeyabharath, P. Veena, M. Rajaram. A novel DTC strategy of torque and flux control for switched reluctance motor drive. **in:** *International Conference on Power Electronics, Drives and Energy Systems, PEDES 06*, 2006, 1–5.
- [8] P. Jinupun, P. Luk. Direct torque control for sensorless switched reluctance motor drives. **in:** *Proceedings of the 7th International Conference on Power Electronics & Variable Speed Drives*, 1998, 329–334.

- [9] L.Venkatesha, V. Ramanarayanan. Torque ripple minimisation in switched reluctance motor with optimal control of phase currents. **in:** *Proceedings of the 1998 IEEE International Conference on Power Electronics Drives and Energy Systems*, 2, 1998, 529–534.
- [10] T. Miller. *Switched Reluctance Motors and their Control*. Magna Physics & Oxford, 1993.
- [11] G. Song, Z. Li, et al. Direct torque control of switched reluctance motors. **in:** *Proceedings of the 2008 IEEE International Conference on Electrical Machines and Systems, ICEMS 2008*, 2008, 3389–3392.
- [12] P. Srinivas, P. Prasad. Torque ripple minimization of 8/6 switched reluctance motor with fuzzy logic controller for constant dwell angles. **in:** *Proceedings of the IEEE International Conference on Power Electronics Drives and Energy Systems*, 2010.
- [13] D. Staton, W. Soong, T. Miller. Unified theory of torque production in switched reluctance and synchronous reluctance motors. *IEEE Transactions on Industry Applications*, 1995, **31**: 329–337.
- [14] M. Wang. Four phase switched reluctance motor direct torque control. **in:** *Proceedings of the 2011 IEEE international Conference on Measuring Technology and Mechatronics Automation*, 2011, 251–254.
- [15] Z. Zhen, W. Terry, C. Juan. Modeling and nonlinear control of a switched reluctance motor to minimize torque ripple. **in:** *Proceedings of the 2000 IEEE International Conference on Systems, Man and Cybernetics*, vol. 5, 2000, 3471–3448.

